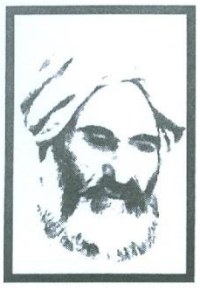

JOURNAL OF SCIENCES

University of Tehran

Abu Reyhan al-Biruni
(973-1048)
Iranian Scientist

ISLAMIC REPUBLIC OF IRAN

ISSN 1016-1104

Vol. 23, No. 3, Summer 2012, Tabestan 1391

CONTENTS

Journal of Sciences, Islamic Republic of Iran 23(3): 231-236 (2012)
University of Tehran, ISSN 1016-1104
http://jsciences.ut.ac.ir

Adsorption Mechanisms of Cadmium onto Pillared Clays and Chalcogenides

M. Razmara and H. Karimi*

Department of Geology, Faculty of Sciences, Ferdowsi University of Mashhad, Islamic Republic of Iran

Received: 29 October 2011 / Revised: 26 June 2012 / Accepted: 12 August 2012

Abstract

Interactions between Cd, pillared clays and chalcogenedies have been studied using nanomineralogical experiments. XRD, DSC and chemical analysis. The synchrotron-based X-ray absorption spectroscopy (XAS) was applied to characterize the reaction phases. The mean bond lengths between, Cd-S, Fe-S, Sb-S, Cd-Cd (in chalcogenedies), Al-Cd, Cd-Ti, and Fe-Cd, (in pillared clays) were determined by XAS method. The ligands information around cadmium atoms was obtained directly from EXAFS and indirect from XANES experiments. Cadmium bearing phases and diffusion of Cd in phases were distinguished by HRXRD, SEM and EPMA. The XAS analysis showed that cadmium sorbed onto pillared clays through a distinct mechanism. These data indicated that the major adsorbent of Cd is a complex of Al, Ti and Fe pillared clays.

Keywords: EXAFS; XANES; SEM; HRXRD; Pillared Clays

Introduction

Cadmium is a fairly mobile element in soils. Cadmium (Cd) is one toxic heavy metal of particular environmental concern, because it can be introduced into and accumulated in soils through agricultural application of sewage sludge, fertilizers, and/or through land disposal of Cd-contaminated municipal and industrial wastes [1].

While pillared clays are commonly used as catalysts, they are also finding applications as novel adsorbents. The advantages of pillared clays include increased surface area and pore volumes, which results in greater adsorption capacity and better flow properties when compared to the unpillared parent clays. Recently, adsorption of a variety of heavy metals onto pillared clays has been reported [2].

Previous research has demonstrated that FeS can be a good reactant/adsorbent to remove selenium from water [3]. As a result, a systematic investigation of the substitution of Cd into the Pillared Clays and chalcogenides was carried out to understand the effect of Cd substitution on the structure of these compounds, and the transformations and reactions of silver chalcogenides. The aim of this study was to optimize the conditions for pillared clays to enhance the adsorption of Cd^{2+} and to compare the adsorption behavior of Cd^{2+} on pillared clays with that of substitution on chalcogenides.

Materials and Methods

The raw materials were collected from two sites, air dried, and crushed to pass through a 200-mesh sieve. The clay used in this study is a bentonite from a deposit of NE of Iran (SE of Sabzevar) but the red mud used for

* Corresponding author, Tel.: +98(913)3063370, Fax: +98(311)3686096, E-mail: h_karimi1398@yahoo.com

Table 1. The chemical analysis (XRF) of montmorilonite, modified montmorilonite and pillared clay

Oxide	Montmorilonite	Modified montmorilonite	Pillared clay	Pillared clay (Acid treatment)
SiO_2	57.49	61.25	13.00	19.98
Al_2O_3	12.57	13.18	13.98	14.35
TiO_2	0.455	0.728	7.17	7.09
Fe_2O_3	3.82	5.87	22.17	40.87
MnO	0.139	0.269	0.06	0.07
MgO	5.18	4.97	2.01	0.43
CaO	1.31	0.24	24.25	3.02
Na_2O	7.98	4.11	4.20	0.38
K_2O	0.37	0.39	0.42	0.27
SO_3	0.003	0.005	1.63	0.07
P_2O_5	0.001	0.002	0.16	0.10
L.O.I	9.11	8.02	9.55	12.41
Total	99.41	99.42	98.60	99.04

Table 2. EPMA of synthetic cadmium–bearing miargyrite and cadmium–bearing smithite compositions

Exp. No.	Weight percent					Total	Experimental formula
	Ag	*Sb*	*As*	*Cd*	*S*		
10SbCd	36.36	38.58	-	3.85	20.68	99.60	$(Ag_{1.05}Sb_{0.98}Cd_{0.11})S_2$
15SbCd	35.00	36.90	-	7.06	20.69	99.88	$(Ag_{1.01}Sb_{0.94}Cd_{0.20})S_2$
20SbCd	34.43	36.44	-	7.76	20.65	99.47	$(Ag_{1.00}Sb_{0.93}Cd_{0.21})S_2$
25SbCd	34.19	36.19	-	8.10	20.83	99.45	$(Ag_{0.98}Sb_{0.92}Cd_{0.22})S_2$
30SbCd	34.02	36.10	-	8.35	20.87	99.25	$(Ag_{0.96}Sb_{0.90}Cd_{0.04})S_2$
10AsCd	32.20	-	34.18	2.19	30.64	100.21	$(Ag_{0.64}As_{0.95}Cd_{0.04})S_2$
15AsCd	36.66	-	24.49	14.19	25.10	100.44	$(Ag_{0.83}As_{0.87}Cd_{0.32})S_2$
20AsCd	28.41	-	20.53	27.52	24.36	100.82	$(Ag_{0.70}As_{0.73}Cd_{0.65})S_2$

pillaring was collected from Jajarm area. Clays are abundant, cheap, negatively charged layered alumino-silicate minerals that make good cationic adsorbents due to their relatively large surface areas. Clays adsorb heavy metals via ion exchange reactions and by the formation of inner-sphere complexes through $\equiv Si\text{-}O^-$ and $\equiv Al\text{-}O^-$ groups at the clay particle edges [4]. At the first, montmorillonite was converted to Na+-exchanged form with 1.0 mol L−1 NaCl and washed until free of chloride. The clay was dried at 105°C. The treated Na^+-montmorillonite was designated Na^+-montmorillonite.

X-ray Powder diffraction techniques were used to identify run products, the purity of phases, to check the structural nature of the reaction products and to obtain unit cell parameters. Experiments were made at room temperature on a Philips PW1730 diffractometer with Ni-filtered Cu Kα radiation (λ = 1.5406 Å) operated at 40 kV and 20 mA. Chemical analyses for the starting clay and its pillared samples were carried out by ICP method. To better understand chemical changes that affect sorption of Cd by sulfides, XAS experiments were carried out at the Daresbury synchrotron radiation source (SRS, UK) operated at 2 GeV with beam current in the range of 120 to 250 mA.

Results and Discusion

The XRD data (as a semi-quantitative method) showed that the red mud contains mainly hematite, calcite, diaspore, gibbsite and katoite. Anatase, quartz and kaolinite are also present as minor constituents. The results of the mineralogical analysis by XRD were also confirmed by SEM observations. The chemical analysis of montmorilonite, modified montmorilonite and

Table 3. X ray powder diffraction data for Pure $AgSbS_2$, 5% Cd and 10% Cd in $AgSbS_2$ phases

Pure $AgSbS_2$				5% Cd in $AgSbS_2$				10% Cd in $AgSbS_2$			
I/I_0	2θ	d_{hkl}	hkl	I/I_0	2θ	d_{hkl}	hkl	I/I_0	2θ	d_{hkl}	hkl
96.03	27.303	3.264	111	0.60	25.898	3.4376		0.43	21.159	4.1955	
100.00	31.630	2.826	200	59.23	27.333	3.2602	111	0.53	21.513	4.1273	
66.96	45.351	1.999	220	100	31.667	2.8332	200	0.34	21.850	4.0644	
28.19	53.802	1.704	311	081	33.266	2.6911		0.84	24.739	3.5959	
18.94	56.404	1.632	222	0.90	36.382	2.4674		1.73	26.679	3.3387	
5.22	26.703	-		0.42	39.720	2.2674		72.95	27.333	3.2603	111
				0.64	41.798	2.1594		100.00	31.670	2.8230	200
				37.23	45.368	1.9974	220	0.45	33.217	2.6949	
				0.55	52.687	1.7359		0.25	34.590	2.5911	
				17.20	53.766	1.7036	311	51.82	45.409	1.9957	311
				10.63	56.353	1.6313	222	0.78	46.135	1.9660	
				0.58	60.718	1.5241		0.73	50.056	1.8208	
				0.43	62.606	1.4826		19.38	53.797	1.7026	
				2.47	66.081	1.4128		6.20	54.000	1.6967	
				6.12	72.899	1.2966		10.88	56.398	1.6301	222
				2.55	73.095	1.2936		1.01	58.071	1.5871	
				0.65	74.356	1.2747		0.61	64.829	1.4370	
								4.72	66.106	1.4123	
								2.14	66.320	1.4083	
								6.77	72.958	1.2956	
								3.49	73.169	1.2924	
								0.59	74.657	1.2703	

pillared clays are listed in Table 1. Pillared clays have high cation exchange capacities that enhance their potential to remove cationic contaminants from aqueous systems. This study has shown that a mixture (30:70) of modified montmorilonite plus pillared clay has a higher capacity for Cd removal than naturally occurring material. Sorption processes at the mineral/water interface typically control the mobility of cadmium compounds.

EPMA the run products for Cd substitution showed different behavior of Cd between high temperature and low temperature forms of $AgSbS_2$. At high temperature, the run products appeared homogeneous up to 5.18 atomic % Cd (Table 2). Substitution of more Cd in the structure of β-miargyrite was accompanied by some CdS in the charges which could not enter in the structure. Excess CdS in the sample indicated that the structure is saturated with Cd, although the Cd-bearing β-miargyrite grains were chemically homogeneous in all samples. EPMA showed that β-miargyrite can accept 4.70 atomic % Cd in the structure as a single phase (Table 2), and up 5.63 atomic % Cd in the presence of excess CdS. In the low temperature α-from more Cd can be accommodated, with 6.77 atomic % Cd as a single phase and 8.12 atomic % in the presence of pyrargyrite (Ag_3SbS_3), stibnite (Sb_2S_3) as well as Cds (Table 2).

X-ray diffraction intensities of the samples were measured at room temperature. Unit cell dimensions were determined by the least-squares refinement of 22 reflections with $15° < 2\theta > 75°$. X ray powder diffraction data for Pure $AgSbS_2$, 5% Cd and 10% Cd in $AgSbS_2$ phases are listed in Table 3.

XRD showed that the substitution of Cd in the structure of β-miargyrite affected the structure of β-miargyrite. Comparison of the XRD patterns of β-miargyrite and Cd-bearing β-miargyrite showed that low contents of Cd (1 atomic%) are accompanied by the shrinking of the (a) lattice (Fig. 1). More Cd (3 atomic%) causes further shortening of cell parameter.

DSC experiments of Cd-bearing β-miargyrite (1 atomic%) showed an exothermic reaction beginning at 277 °C imply that the transition from the metastable

cubic phase to a lower symmetry phase has been delayed in comparison to that in pure β-miargyrite (Fig. 2). Note that even very small amounts of Cd can affect the temperature of the heat effect. Another event at 349 °C is most likely related to the transformation of matastable intermediate phase to the stable monoclinic phase. An endothermic reaction starting at 369 °C can be correlated with the phase transition from the monoclinic form of cadmium–baering miargyrite (in compare of pure monoclinic miargyrite) to the high temperature cubic form. This event has occurred at a lower temperature than the phase transition for pure miargyrite. A weak endothermic reaction beginning at 465 °C suggests the presence of another metastable form of cadmium–bearing miargyrite. Addition of more Cd (~3 atomic%) causes more distortion in the structure, consequently, the first exothermic peak has increased to 299°C. As increasing Cd substitution causes greater distortion of the structure framework of miargyrite this retardation was expected, but substituting more than 5 atomic %Cd appears to have changed the structure of Cd-bearing β-miargyrite singnificantly and therefore the exothermic peak appeared at 217 °C. Higher Cd substitution might cause an earlier phase transition from distorted Cd-bearing miargyrite to β-miargyrite form as suggested by a small peak at 366.90 °C. Such relationships might indicate that greater substitution of Cd into β-miargyrite causes weaker bonding between atoms and more readiness of the phase to become distorted. Substitution of more Cd in the structure of β-miargyrite systematically decreased the temperature of the phase transition (Fig. 2).

EXAFS studies for Cd substituted in Sb or Ag sites in β-miargyrite provided information on the Cd and Ag present in the structural environment of $AgSbS_2$. Ag-k-edge EXAFS spectra for Cd-bearing β-miargyrite are shown in Figure 3. Comparsion of the Ag k-edge EXAFS studies of β-miargyrite and Ag K-edge EXAFS in Cd-bearing β-miargyrite showed that the Ag-S bond length of Cd-bearing β-miargyrite has decreased from 2.83 Å in pure β-miargyrite to 2.53 Å in Cd-bearing β-miargyrite (~5 atomic %). A good spectra resemblance was observed between the two samples (Fig. 4), indicating a similar structural environment for the two metals. Cd K-edge EXAFS showed the coordination number to be 6.4 which is within error of the real coordination number of 6 (Table 4). The XANES analysis showed that cadmium sorbed onto pillared clays through a distinct mechanism. These data indicated that the major adsorbent of Cd is a complex of Al, Ti and Fe pillared clays.

As a result, the a-cell parameter of β-miargyrite decreases with increasing amount of Cd (Compae with the XRD patterns). This phenomenon shows that the M(Ag, Sb)-S bond is compressed and the structure has distorted from the ideal cubic form. Table 5 shows the effect of Cd substitution in the bond length and co-ordination number of α-miargyrite.

The Debye-waller factor for the first shell of S atoms surrounding Cd in Cd-bearing β-miargyrite is bigger than for Ag atoms in pure β-miargyrite, suggesting that the Ag environments in Cd-bearing β-miargyrite are more disordered.

A more quantitative measure of local disorder can be obtained by observing the width of a peak corresponding to a particular coordination shell in the Fourier transform, wider peaks indicate a greater range

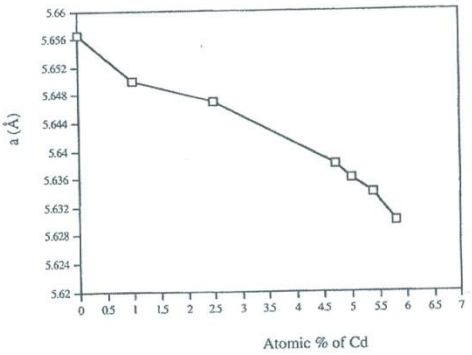

Figure 1. The variation in the lattice parameter (a) of cadmium–beraing β-miargyrite as a function of Cd content.

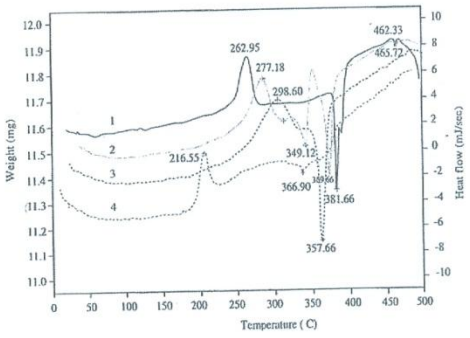

Figure 2. DSC curves for synthetic cadmium–bearing β-miargyrite: (1) pure β-miargyrite, (2) 1 atomic% cd substituted in β-miargyrite, (3) 3 atomic % Cd substituted in β-miargyrite, (4) more than 5 atomic % Cd substituted in β-miargyrite.

of radial distances and higher static or thermal disorder. Refined Ag K-edge EXAFS data for β-miargyrite showed wider peaks for Cd-bearing - β-miargyrite than for pure β-miargyrite. This clearly indicates that Cd-bearing β-miargyrite is more disordered than pure β-miargyrite.

The structural parameters obtained for Cd atoms showed that Cd substitutes for Ag and Sb in crystallographical sites. In the Cd-site, the charge compensation could occur by a combined substitution of univalent Ag and trivalent Sb. The greater distances of Cd-S (2.59 Å) in Cd-bearing β-miargyrite in comparison to Ag-S (2.53 Å) and Sb-S (2.40 Å) in β-miargyrite can be interpreted by a dual role for Cd.

Cd k-edge EXAFS was also used to investigate the structural environment of Cd present in α-$AgSbS_2$. At lower temperatures, the substitution of Cd in Ag sites of α-miargyrite changes the bond length to 2.47 Å and Coordination number to 3.

Schapbachite ($AgBiS_2$) and β-miargyrite ($AgSbS_2$) are isomorphous phase. Both of them have a cubic from at high temperatures. Because $AgSbS_2$ accept Cd in its structure an attempt was made to substitute Cd into $AgBiS_2$. The starting compositions with up to 5 atomic% Cd in $AgBiS_2$ were synthesized. The products were 100% (Ag, Bi, Cd)S_2 showing that the limit of Cd substitution had not been reached. Substitution of Cd causes the unit cell schapbachite to decrease in volume (Fig. 5), but it remains cubic with a cell parameter decreasing to ~5.618 Å when atomic 5 atomic% Cd is present (Table 3).

The results of XAS experiments showed that despite the smaller difference in ionic radius between Bi and Cd than between Sb and Cd, $AgBiS_2$ can accept less Cd in its structure than $AgSbS_2$. The reason for this different is likely to be related to fundamentally different phase relations shown by the Ag_2S-Bi_2S_3 and Ag_2S-Sb_2S_3 systems. Also, in the phase transition from cubic schapbachite to hexagonal matildite, the possibility of bond bending increases and therefore high Cd-solubility is expected. However the differences in ionic size of Cd (0.95 Å), Bi (1.03 Å) and Ag (1.15 Å) are factors which will restrict the solubility of Cd in matidite.

The small atomic radius and non-metalic character of arsenic suggest that Ag^+ and As^{3+} can not be easily substituted by Cd^{2+}. Attempts to synthesis Cd-smithite produced very inhomogeneous charges containing $AgAsS_2$ with a very large range of Cd-contents. Locually up to 28 wt% Cd were recorded but in the same sample values below 0.5 wt% Cd were observed. Examination by SEM indicated fine intergrowths of phases, perhaps $AgAsS_2$ and CdS. Attempts to substitute cadmium in $AgAsS_2$, showed that the substitution was only possible in very small amounts. Higher cadmium contents in the starting compositions produced unmixing of a soild solution and exsolution observed by SEM.

EPMA and SEM analysis showed that exsolution processes in smithite occur mainly as a result of the change in the extent of solid solution between Cd-poor

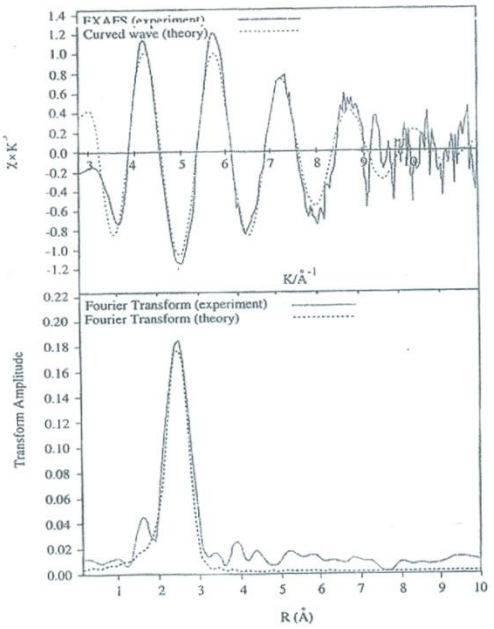

Figure 3. Ag K-edge EXAFS (top) and Fourier transform (bottom) of Cd – bearing β-miargyrite.

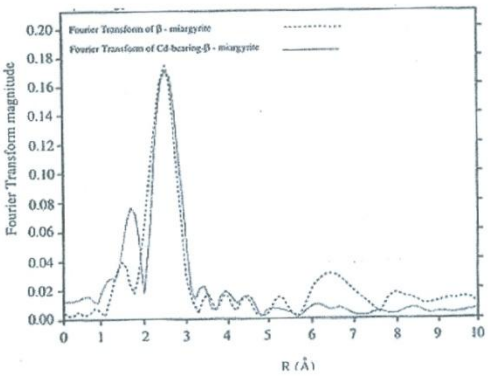

Figure 4. A comparsion of Fourier transform between the Cd K-edge in Cd bearing β-miargyrite and Ag K-edge EXAFS in β-miargyrite.

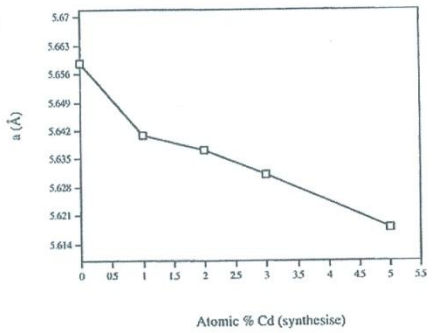

Figure 5. Cell parameter (a) change for the composition in synthetic Cd-bearing schapbchite.

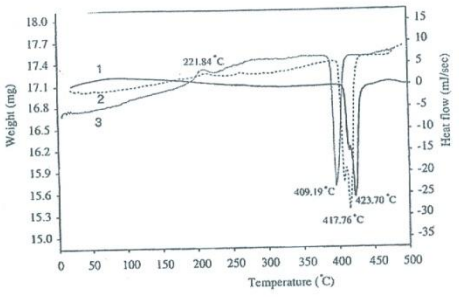

Figure 6. DSC curve for synthetic and cadmium–bearing smithite, 1) pure smithite, 2) (Ag, As, Cd)S_2 containing 0.3 atomic% Cd substituted in smithite and 3) inhomogeneous sample with high Cd-content (>5 atomic % Cd).

Table 4. Comparsion of EXAFS parameters for the Ag K-edge, Sb K-edge and Cd k-edge in Cd-bearing β-miargyrite and β-miargyrite

6%Cd-bearing β-miargyrite				β-miargyrite		
bond	R	C.N.	D.W.	R	C.N.	D.W.
Ag-S	2.53	1.5	0.027	2.55	3	0.041
Sb-S				2.40		0.01
Cd-S	2.59	6.4	0.031			

R = Average M(Ag, Sb)-S scatter bond length ± 0.020 Å
D.W. = Debye-waller factor, $2\sigma^2$ (±0.004 Å^2)

Table 5. Comparsion of EXAFS parameters for the Ag K-edge, Sb K-edge and Cd k-edge in Cd-bearing α-miargyrite and α-miargyrite

6%Cd-bearing α-miargyrite				α-miargyrite		
bond	R	C.N.	D.W.	R	C.N.	D.W.
Ag-S				2.47	3	0.056
Cd-S	2.55	4.1	0.029	-	-	-
Cd-S	3.87	12	0.66			

R = Average M(Ag, Sb)-S scatter bond length ± 0.020 Å
D.W. = Debye-waller factor, $2\sigma^2$ (±0.004 Å^2)

and Cd-rich $AgAsS_2$ at determined temperatures. Mechanisms of exsolution may be relevant to homogeneous nucleation over a relatively restricted range and heterogeneous nucleation operates in most of the system.

DSC experiments showed that the Cd content affects the melting point and the possible phase transition of smithite (Fig. 6). low-content Cd (0.3 atomic%) reduces the melting temperature by 6 °C to 418 °C. The inhomogeneous sample which must contain $AgAsS_2$ structure with Cd has and even lower melting point. However it is noted that in the peak for the 0.3 atomic % Cd sample, evidence of a phase transition just prior to the melting point is observed. This may be evidence of the third structural form of smithite. A very strong reaction beginning at 409 °C is probably related to the melting point of smithite.

The results of the investigations about adsorption of cadmium onto pillared clay can be summarized as following:

– The EXAFS and XANES results indicated that little or no structural change occurs in the clay host upon intercalation of the pillaring agents.

– The data reveal that cadmium adsorption is influenced by the type of adsorbent, particle size, pH and the presence of calcium and sulfur. Sorption processes at the mineral/water interface typically control the mobility of cadmium compounds.

– This study has shown that a mixture of modified montmorilonite plus pillared clay has a higher capacity for Cd removal than naturally occurring material. The study results suggest that pillared red mud (modified montmorilonite plus red mud) could be a new type of environmental adsorbent for cadmium in contaminated waters.

References

1. D'Souza L., Devi, P., Shridhar, M.P., Naik C.G. Use of Fourier Transform Infrared (FTIR) Spectroscopy to Study Cadmium-Induced Changes in Padina Tetrastromatica (Hauck), *Analytical Chemistry Insights*, **3**: 135-143, (2008).
2. Saha, U. K., Taniguchi, S. and Sakurai, K. Simultaneous adsorption of cadmium, zinc, and lead on hydroxy-aluminum- and droxyaluminosilicate- montmorillonite complexes, *Soil Sci. Soc. Am. J.* **66**: 117–128, (2002).
3. Batchelor, B., Han, D. S. and Kim, E. J. Novel Adsorbent-Reactants for treatment of ash and scrubber pond effluents, US Department of Energy (DOE), National Energy Technology Laboratory (NETL), (2010).
4. Barbier, F., Duc, G. and Petit-Ramel, M. Adsorption of lead and cadmium ions from aqueous solution to the montmorillonite: water interface, *Colloids Surf. A.* **166**: 153–159, (2000).